

## Optimal Design of Three-Phalanx Prosthesis Underactuated Fingers Using Genetic Algorithm

**Dr. Sadeq H. Bakhy**

Machines and Equipment Engineering Department, University of Technology/Baghdad  
Email: sadeqbakhy@yahoo.com

**Dr. Shaker S. Hassan**

Machines and Equipment Engineering Department, University of Technology/Baghdad

**Dr. Somer M. Nacy**

Al-Khwarizmi College of Engineering, University of Baghdad/Baghdad

**Dr. Alejandro Hernandez-Arieta**

Artificial Intelligence Laboratory, University of Zurich. Switzerland

**K. Dermitzakis**

Artificial Intelligence Laboratory, University of Zurich. Switzerland

Received on: 15/12/2011 & Accepted on: 8/11/2012

### ABSTRACT

This research is interested to investigate the optimum design procedure for a finger driving mechanism to have a proper configuration of the finger for its utilization in hand prosthesis. To get this goal, a Genetic Algorithm (G.A) was used. Three criteria were selected to find the optimal solution. The most important of them was the percentage of the grasping stability. This criterion was evaluated as must type by using Kepner-tregos method. When the optimal solution was found, this one was modified to facilitate the fabrication of a prototype. The modifications consist of mostly rounding the parameters and uniforming the rollers dimensions. Those changes did not affect too much the forces characteristics. The prosthetic hand prototype was built of hard ABS (Acrylonitrile Butadiene Styrene) plastic using rapid prototyping. Testing results indicate that the proposed Genetic Algorithm gives reasonable -quality results in short computation time.

**Keywords:** Genetic Algorithm, Three-Phalanx Prosthesis, Underactuated Fingers.

التصميم الامثل للاصابع الصناعية المخفضة التشغيل ذات ثلاث سلاميات باستخدام الخوارزمية الوراثية

### الخلاصة

يهتم هذا البحث بالتحقق عن اسلوب التصميم الامثل لالية تحريك الاصابع للحصول على شكل ملائم للاصابع عند استخدامه في اليد الصناعية. للوصول لهذا الهدف , استخدمت الخوارزمية

الوراثية. تم اختيار ثلاث معايير لايجاد الحل الامثل. وكان الاكثر اهمية من بينها النسبة المئوية لاستقرار القبضة. وتم تصنيف هذا المعيار من النوع الالزامي باستخدام طريقة كينر-تريكوز. وعند ايجاد الحل الامثل, تم تعديل ابعاد الاصبع ليلائم تصنيعه كأمودج. تضمنت معظم التعديلات تقريب المعاملات وتجانس ابعاد المدحرجات, ولم تؤثر تلك التغيرات كثيرا على خصائص القوى. تم تصنيع أمودج اليد الصناعية من مادة ABS اللدائنية المصعدة بأستخدام النمذجة السريعة. أظهرت نتائج الاختبارات بأن الخوارزمية الوراثة المقترحة تعطي نتائج ذات نوعية عالية في زمن حسابي قصير.

## INTRODUCTION

A human hand is a complex structure having 21 degrees of freedom (DOF): Four DOF per finger which has three phalanges and one metacarpus and five DOF for the thumb which has two phalanges and one metacarpus. Figure (1) shows a hand physiology [1]. It can perform grasping, holding and pinching operations while manipulating objects of various sizes, weights and shapes. To mechanically simulate these functions, planar mechanisms with one DOF are generally used in mechanical hands [2].

Commercially prosthetic hands, such as Otto Bock Hand™ [3], are limited to a single degree of freedom (DOF) in their movement. Traditionally a single motor drives the first and second fingers of the hand in unison with the thumb to produce a tri-digital grip. The remaining two fingers on the hand are for aesthetic purposes and move passively with the first two fingers.

Carrozza et al. [4] presented an underactuated artificial hand intended for functional replacement of the natural hand in upper limb amputees. The architecture of the hand comprised the following modules: an actuator system embedded in the underactuated mechanical structure (artificial muscoskeletal system), a proprioceptive sensory system (position and force sensors), and an exteroceptive sensory system, and an embedded control unit. The hand was underactuated (9 degrees of freedom controlled by two actuators) and was equipped with an opposable thumb and a proprioceptive sensory system. the maximum measured grasping force was 18N.

Pons et al. [5] introduced an outline of the main details of the mechanical design and control aspects of the MANUS-HAND prototype. The number of active joints was more than tripled as compared to commercial prostheses, and up to four grasping modes (cylindrical, precision, hook and lateral) were available with just two actuators. They adopted an underactuated kinematics concept to keep the system complexity, size and, weight within reasonable limits. The total weight of the prototype was 1.2 kg, this is, in fact, over the specifications.

Pylatiuk et al. [6] presented an experimental hand prosthesis design to increase functionality by using an electrohydraulic drive system, a new experimental prosthetic hand. However, the weight was comparable to that of a conventional prosthesis with one degree of freedom. In order to move the center of mass closer to the body, the hydraulic pump can be outside the hand. As a result, the stresses on the remaining limbs are reduced, and the prosthesis is felt lighter.

Kevin et al. [7] described the design of 21 degrees-of freedom, nine degree-of-actuation, gas-actuated arm prosthesis for trans-humeral amputees. The arm incorporated a direct drive elbow and three degree-of-freedom wrist, in addition to a 17 degrees-of-freedom underactuated hand affected by five actuators. The anthropomorphic device included full position and force sensing capability for each actuated degree of freedom and integrated a monopropellant-powered gas generator to provide on-board power for untethered operation.

Jung et al. [8] presented a biomimetic robotic hand with tendon-driven three fingers with performance and flexibility as the human hand. Each finger could control one independent flexion motion by the one tendon and one DC motor. And, the rotation motion of thumb was performed by one actuator. The extension motion of finger was implemented by a restoration spring. The robotic hand with tendon-driven three fingers, was composed of the thumb, the index, and the middle fingers and it had totally 4-DOF because of the hand was actuated by four actuators. The robotic hand with tendon-driven three fingers performed six hand functions, such as the direction, the scissors, the rock, the precision grasp, the tip grasp, and the lateral hip. In order for the previously described parameters to be met optimum sizing of finger driving mechanisms by using fundamental characteristics regarding with the human-like behavior, grasp efficiency and force transmission, identification solution based on the Genetic Algorithm (GA) was proposed in this study. However, significant efforts have been made to find designs that are simple enough to be easily built and controlled in order to obtain practical systems, particularly in human prosthetics.

### **FORCE PROPERTIES OF THREE-PHALANX UNDERACTUATED FINGERS THEORY**

Some assumptions were made on the Finger architecture and the contact, namely negligible friction at the contacts. The object will be assumed fixed with respect to the base of the finger and the local geometry of the contacts will also be neglected, i.e., a single fixed point of contact on each phalanx is assumed.

Geometric details and nomenclature of the finger using a tendon-actuated finger models are provided in Figure (2), which can be written as [9, 10];

$$f = J^{+T} T^{-T} t \quad \dots (1)$$

Where  $f = [f_1 \quad f_2 \quad f_3]^T$  is the vector of the normal contact forces, and  $J$  is a lower triangular matrix characterizing the contact locations that can be expressed analytically, one has:

$$J = \begin{bmatrix} k_1 & 0 & 0 \\ k_2 + l_1 \cos \theta_2 & k_2 & 0 \\ k_3 + l_1 \cos(\theta_2 + \theta_3) + l_2 \cos \theta_3 & k_3 + l_2 \cos \theta_3 & k_3 \end{bmatrix} \quad \dots (2)$$

The transmission matrix  $T$  characterizes the underactuation for a finger using a tendon-actuated finger, one has:

$$T = \begin{bmatrix} 1 & -\frac{r_2}{r_1} & -\frac{r_2 r_4}{r_1 r_3} \\ 0 & 1 & 0 \\ 0 & 0 & 1 \end{bmatrix} \quad \dots (3)$$

Where  $r_{2i-1}$  and  $r_{2i}$  for  $i > 0$  are the radii of the pulley located at the base and the end of the  $i$ th phalanx. and,

$$f_1 = \frac{(U' Ta)}{k_1 k_2 k_3 r_1 r_3} \quad \dots (4)$$

$$f_2 = \frac{-r_2(-k_3 r_3 + r_4 l_2 \cos \theta_3 + r_4 k_3) Ta}{k_2 k_3 r_1 r_3} \quad \dots (5)$$

$$f_3 = \frac{r_2 r_4 Ta}{r_1 r_3 k_3} \quad \dots (6)$$

With

$$U' = l_1 r_2 \cos \theta_2 (r_4 l_2 \cos \theta_3 + (r_4 - r_3) k_3) - l_1 r_2 r_4 k_2 \cos(\theta_2 + \theta_3) + (r_1 - r_2) k_2 k_3 r_3 \quad \dots (7)$$

By using the equations (4) to (7), it is possible, for a given posture of the Finger and a given contact situation, to determine the contact forces on the phalanges and therefore assess the force transmission characteristics of the Finger.

If all the contact forces are positive, then the configuration of the Finger is the one depicted in the last schematic of the ideal grasping sequence in tow dimension is visualized in Figure (3). The ideal grasping sequence may not always occur and some sequences may instead lead to the ejection phenomenon illustrated in Figure (4) [10]. Thereupon, in this configuration, some forces may be negative. The case where the three forces are negative is not very likely to happen.

### **OPTIMIZATION OF THE DESIGN**

Now, one is now interested to have a good configuration of the finger for its utilization in hand prosthesis. Because the main task of this finger is to grasp objects (so to apply forces to them), it's normal to do the optimization in function of forces criteria. It is very difficult, in the static model (equations (4) to (7)) to isolate each parameter because of the complexity of the system, and to solve the problem, a

genetic algorithm was used. The main components of a genetic algorithm for prosthesis robotic hands are as follows [11]:

**Solution Encoding**

The solution is represent by the string (vector) of ten parameters(see the Table 1), while these parameters (known as genes) are joined together to form a string of values (often referred to as a chromosome). The fingers of the hand prosthesis must be covered by a cosmetic glove. Moreover, the optimization is a function of the size of the hand, so the size of the glove. Here, a glove of the company Otto Bock was used to define the parameters boundaries [12].

**Initial Population**

The initial population of chromosomes is created by random methods, i.e., those 10 parameters were all defined should satisfy the numerical values of the boundaries to avoid any interference between the parts (phalanxes, string, etc.) inside the cosmetic glove.

**Fitness Function**

The measurement of parameter (chromosome) is based on the objective function (fitness).When a population is generated, each chromosome is evaluated, and its fitness is calculated for each parameter. Finally, each chromosome is assigned its fitness value along of the population size. As said before, the main task of the finger is to grasp, then those criteria are derived from the model (equations(4) to(7)). Those criteria were defined to find the parameters.

**First criterion: The percentage of the grasping stability**

Concerning the contact forces, when these forces are negative, the associated phalanx will move in a clockwise direction, which gets away from the object (Ejection, illustrated in Figure (4)). To characterize the capability of the underactuated finger to create full-phalanx grasps with an index [10],

$$I_{per} = \frac{\int_W \delta(\theta^*, k^*) dk^* d\theta^*}{\int_W dk^* d\theta^*} \quad \dots (8)$$

where  $\delta(\theta^*, k^*)$  is a Kronecker delta symbol for positive of  $f$  vector that eliminates non-whole-phalanx grasps:

$$\delta(\theta^*, k^*) = \begin{cases} \mathbf{1} & \text{if } \mathbf{f}_i > \mathbf{0} \quad i = 1, 2, 3 \\ \mathbf{0} & \text{otherwise} \end{cases} \quad \dots (9)$$

And  $W$  is the workspace of the finger in terms of  $(\theta^*, k^*)$ , i.e., the hyper parallelepiped defined by  $l_i > k_i > 0$  &  $\frac{\pi}{2} > \theta_i > 0$ ,  $i > 0$ . This index physically represents the percentage of the stability that is achievable by full-phalanx grasps, namely, whole-hand grasping workspace.

**Second criterion: The grasp forces**

The forces should be well distributed among the phalanges of prosthetic hand in order to avoid large local forces on the object. The corresponding index is defined

as the ratio of the total force on the three phalanges divided by the largest force, namely

$$I_{gs} = \frac{f_1 + f_2 + f_3}{\max(f_i)}, \quad \forall \theta_i, \quad i = 1,2,3 \quad \dots (10)$$

**Third criterion: Maximum pinching force**

To assure the stability of the grasp, one needs a certain pinching force. This force should be as high as possible, so

$$I_{mpf} = \frac{(f_1 + f_2 + f_3)_{max}}{F_a}, \quad \forall \theta_i, \quad i = 1,2,3 \quad \dots (11)$$

**Selection(Reproduction)**

Reproduction is a process in which individual strings are copied according to their objective (fitness) function values. For instance, the fitness of an organism is typically defined as the probability that the organism will live to reproduce or as a function of the number of offspring the organisms has (fertility).

**Genetic Operators**

Genetic Operators (crossover and mutation) applied to the chromosomes whose role is to create new members, i.e., children, in the population by crossing the genes of two chromosomes (crossover operators) or by modifying the genes of one chromosome (mutation operators):

**a) Crossover:**

Crossover is the exchange of genes between the chromosomes of the two parents. In the simplest case, one can realize this process by cutting two strings at a randomly chosen position and swapping the two tails. This process, which is called two-point crossover, is visualized in Figure (5).

**b) Mutation:**

The role of a mutation operator is to provide and maintain diversity in a population so that other operators can continue to work. Typically, in a simple GA system, researchers generally use on the order of one mutation per thousand bit (position) transfers (the probability of 0.001), or less.

**Replacement**

Natural selection of the members of the population, who will survive (replacement), is based on elitism. That is to keep the best chromosomes of the current population and their offspring. They will form a new population to survive into the next generation.

**Parameter Selection**

Natural convergence of the whole population is globally improved at each step of the algorithm for choosing suitable values of parameters, such as population size

and crossover. The performance of a (GA) depends largely on the design of the above components and the choice of parameters such as population size, probabilities of genetic operators (i.e., crossover and mutation), and number of generations.

**The decision making:**

Kepner-tregos method is used to facilitate the decision-making process and make trade-offs between solutions or proposed solutions to a particular hand prosthesis. This method is similar to a large extent to the gradient weighted method  $\Sigma G.W$  [13] but the fundamental difference is the presence of another parameter for the property in addition to the standard value weighted ( $W$ ), a measure important for the property (criteria) can be illustrated in the following step:

1. Definition and scheduling features or requirements that will be through a process of differentiation and decision-making, depending on the properties listed in table measure of value design .

2. Criteria are classified into two categories according to importance, namely :

i. **The first category:** the criteria that must be imposed are called (must), and these criteria are not taking the weighted given in the table for measure the design values. For this work, a prosthetic hand design must encompass the first criteria to prevent the phalanx movement in a clockwise direction which gets away from the object.

ii. **The second category:** it is required to achieve the criteria called (want), and these criteria in order of value weighted ( $W$ ) are taken from the table (2) of design value measure. In fact, the second criteria is most important than the third criteria, Then, each of want criteria was expressed in a unitary scale (where 0 is the worst value and 1 is the best one). After, a weight factor was given to each want criteria to give them more or less importance.

Note that the sum of the weight factor must be one ( $\Sigma W = 1.0$ ).

3. The definition of solutions.

4. An evaluation of these solutions for the properties imposed on (must) and the required properties (want). To simplify the assessment process for the properties imposed, the words (Go) can be written under the solution that verifies properties imposed, and the word (No Go) can be set under the solution that do not meet one of the properties imposed.

5. The solution that best matches the properties imposed, and is a better one. For solutions that meet the properties imposed on (must) are evaluations against the required properties (want) using the gradient weighted method  $\Sigma G.W$ . Where,  $G$  is a numerical value for each property (want), and this value indicates the extent of gain or the achievement of each property proposed by the amount of weighted value of each property ( $W$ ), then multiply the total gain ( $G$ ) by the value weighted ( $W$ ) to get the  $\Sigma G.W$ , and put this amount at the end of the Table (2). The solution, which has the highest total of  $\Sigma G.W$ , is considered the best idea of this work.

**COMPUTER PROGRAMMING**

Computer program has been developed by using Matlab 7.8(2009a) program [14]. The program's flow chart that illustrates our proposed methodology of solution is shown in Figure (6).

## RESULTS AND DISCUSSION

The optimization was performed using different population sizes (from 100 to 1000) and different number of generations (from 10 to 1000). All the optimizations used a variation of  $\theta_2$  and  $\theta_3$  from 0 to 90°. This seems to be a reasonable workspace for this application of the finger. A comparison of the results of the four most interesting cases (solution 1, 2, 3, and 4) are presented in table (3), the parameters found by the optimizations and table (4) for the statistical data of the forces. Note that the graphs of the contact forces ratio  $\frac{f_1}{f_a}$ ,  $\frac{f_2}{f_a}$ ,  $\frac{f_3}{f_a}$ ,  $\frac{f_1+f_2+f_3}{f_a}$  and associated stability loci as function of the generalized coordinates for each of these solutions are included in Figures (7) to (10).

An evaluation of these four solutions for the properties imposed on, are considered as (must) and the required properties are considered as (want). The words (No Go) under the solution (Sol. 2) do not meet the first criteria imposed. Because of the contact force of first phalanx ( $f_1$ ) is negative, then the associated phalanx will move in a clockwise direction and gets away from the object. Therefore the percentage of the grasping stability is not 100% (i.e.,  $I_{per} = 0$ ). Finally, the solution (Sol. 2) will be cancelled, as shown in table (5).

The remaining solutions (Sol.1, Sol.3 and Sol. 4) meet the criteria imposed on (must), hence they will be evaluated against the required properties (want) and by using the gradient weighted method  $\Sigma G.W$ . Each of those criteria was expressed in a unitary scale (where 0 is the worst value, and 1 is the best one). After, a weight factor was given to each criterion to give them more or less importance. Indeed, the second criterion is the most important criterion than third criterion since this was the main criteria to select a solution. The grasp forces were evaluated using table (2). One can see that solution 1 has the largest  $I_{gs}$  (i.e.,  $I_{gs} = 2.555$ ). Thus, the performance total  $\Sigma G.W$  will have maximum value ( $\Sigma G.W = 55$ ). Also, the grasping forces were evaluated using the standard deviation (s.d.) (see Table (4)). One can see that solution 1 has the smallest s.d. (4.22%). Moreover, this solution has interesting parameters. Firstly, the value of position of contact forces  $k_1, k_2$ , and  $k_3$  is more accepted than other solutions. Secondly, the forces are more well distributed among the phalanges in order to avoid large local forces on the object. For above reasons, solution 1 was preferred and declared "the optimal solution".

As stated before, the goal of this optimization is to find a good solution. Therefore, to facilitate the fabrication of the hand prosthesis prototype, the optimal design was modified. A table (6) shows the comparison of the parameters between solution 1 and solution 1 modified, and table (7) presents the statistical data.

Firstly, the rollers ( $r_1, r_3$ ) are modified to have equal radius; this is more easy to fabricate. Secondly, some parameters ( $l_1, l_2, l_3, r_2, r_4, k_1, k_2$  and  $k_3$ ) were rounded.



As a consequence of that, one can see from Table (8) that the mean of forces ratio ( $f_1/fa$ ), ( $f_2/fa$ ) and ( $f_3/fa$ ) has increased, while  $I_{gs}$  is decreased. Finally, because the global index ( $\Sigma G.W$ ) remained a significant, the modified design is then better in the sense, and it is easier to fabricate. Figure (11) exhibits the different grasping forces ratios  $\frac{f_1}{fa}, \frac{f_2}{fa}, \frac{f_3}{fa}, \frac{f_1+f_2+f_3}{fa}$  and associated stability loci as function of the generalized coordinates for this modified design.

### **MANUFACTURING OF PROSTHETIC HAND PROTOTYPE**

The prosthetic hand prototypes developed in the work were built of hard plastic using rapid prototyping. This technique allowed the fabrication and demonstration of the prototypes within a short period of time by using 3D Printers machine (see the figure 12). 3D Printers give us the ability to easily test product designs using models made of durable ABS (Acrylonitrile Butadiene Styrene) plastic. Prototypes made of ABS plastic are tough enough to be used as working parts. Complex assemblies can make this work. Pieces formed by dimension actually snap or fit together. ABS prototypes can withstand rigorous functional testing and retain their exact dimensions. The large build capacity of the Dimension 3D printers (model 1200es) has the room to print large functional for evaluation and testing under real-world conditions. The printers are simple to operate too: just click “print” to prep the file in Solid work program (see Figure 13) and print the model, and then remove the support material to reveal the design in three dimensions.

Catalyst® EX software is an intuitive, user-friendly application designed to interface with Dimension 3D printers. STL files are imported into Catalyst® EX Software which automatically slices and orients the parts (see Figure 14a ) and creates any necessary support structures (see figure14b,c). The software automatically plots a precise deposition path for dimension to follow. ABS plastic (in filament form within auto-loading cartridges) is fed into an extrusion head, heated to a semi-liquid state, and accurately deposited in layers as fine as 0.178 mm thick. After completion of the build, support structures are simply removed. ABS plastic is heated to a semi-liquid state and deposited in thin layers by extrusion head (see the Figure 14d). Catalyst software automatically determines when and where to deposit ABS or support material throughout the build process. Dimension 3D Printers are network devices. The critical components (e.g., the guiding pins and springs) are made of metal. The prototypes developed were equipped with a handle in order to provide the manual actuation of the hand, as shown in Figure (15).

It should to be noted that the cylindrical and precision are possible in hand prostheses commercial [3]. In Figure (16) a series of examples of grasps that were performed with the underactuated hand prosthesis are shown. The grasps are generally firm and stable and have a human-like appearance. The hand performed well for enveloping grasps, which involve contact with all the phalanges. However, the hand often performed poorly with pinch grasps of small objects, which involve contact with only the tip of the fingers. The result is an effective, light, and compact hand that is capable of grasping a broad variety of objects. With the recent advances

in prosthesis and humanoid robotics, it is also believed that the concept presented in this work can be very useful in human-like robots. The innovative concept of the four fingers and thumb based on the tendon mechanism allows both opposition and flexion with just one handle actuator.

### **CONCLUSIONS**

1. The design of underactuated finger seems to be very interesting for a hand prosthesis use. The simplicity of the design and its self-adaptation to different shapes of objects are some qualities that give it a good chance to be successful in prosthetics. Hoping that such a design could enjoy the arm defected persons,
2. By using the Genetic Algorithm with the Matlab 7.8(2009a)-software, it is possible to identify all the necessary parameters of the complex mathematical models in a short computation time.
3. The design of underactuated hand seems to be very interesting for a hand prosthesis use. The simplicity of the design and its self-adaptation to different shapes of objects are some qualities that give it a good chance to be successful in prosthetics. Hoping that such a design could enjoy the arm defected persons, and that they would appreciate to use it all day long, even while they sleep.
4. This paper has presented and analyzed the force capabilities of underactuated fingers of a three-phalanx finger considering geometry of the contact and optimal phalanx force distribution, by using a genetic algorithm. An optimization was done to find a good configuration of the parameters of the finger. The design problem has been formulated as a multi-objective optimization problem. The numerical procedure is characterized by fairly simple formulations for the optimality criteria and no great computational efforts in order to achieve practical optimal design solutions. To ensure a stable grasp, ejection must be prevented.

As a future work which can be extended to the control of grasping for robotic hand. It is planned to apply genetic algorithms to different applications to study the controllability of an underactuated hand based on these results.

### **ACKNOWLEDGMENTS**

The authors would like to acknowledge Prof. Rolf Pfeifer, a director of the Artificial Intelligence Laboratory, Department of Informatics, University of Zurich, Switzerland, for his help and assistance. Great thanks to Dr. Thomas Schweizer for his help and allowing me to test the fingertips in the laboratory in Institute Polymer Physics - Swiss Federal Institute of Technology (ETH) in Zurich, Switzerland. This research was partially supported by the Swiss National Foundation Project #CR23I2\_132702/1. Thanks are also to the Ministry of Higher education and Scientific Research – Iraq.

### **REFERENCES**

- [1].AndrisFreivalds, “Biomechanics of the Upper Limbs: Mechanics, Modeling, and Musculoskeletal Injuries”, CRC Press LLC, 2004.
- [2].Vinet, R., Y. Lozach, N. Beaudry and G. Drouin, "Design methodology for a multifunctional hand prosthesis.", *J. Rehabil. Res. Dev.*, 32: 316-324, 1995. <http://www.ncbi.nlm.nih.gov/pubmed/8770796>
- [3].Otto Bock Orthopedic Industry GmbH, Myobock-Arm Components 1997/98, 1997, Otto Bock.
- [4]. Carrozza, M.C. E Vecchit, E Sebastiani, G. Cappiello, S. Roccella, M. Zecca, R. Lazzarini, and P. Dario, “Experimental Analysis of an Innovative Prosthetic Hand with Proprioceptive Sensors”, *Proceedings of the 2003 IEEE International Conference on Robotics & Automation*. Taipei, Taiwan, September, pp.14-19, 2003.
- [5]. Pons,J.L. E. Rocon, and R. Ceres, “The MANUS-HAND Dexterous Robotics Upper Limb Prosthesis”, *Mechanical and Manipulation Aspects, Autonomous Robots*, 16, pp.143–163, 2004.
- [6]. Pylatiuk, C. S. Mounier , A. Kargov, S. Schulz, and G. Bretthauer, “Progress in the Development of a Multifunctional Hand Prosthesis”, *Proceedings of the 26th Annual International Conference of the IEEE EMBS, San Francisco, CA, USA*. September, pp.1-5, 2004
- [7].Kevin T. O’Toole, and Mark M. McGrath. “Mechanical Design and Theoretical Analysis of a Four Fingered Prosthetic Hand Incorporating Embedded SMA Bundle Actuators”, *International Journal of Mathematical, Physical and Engineering Sciences*, Volume 1, Number 2, 2007.
- [8].Sung-Yoon Jung, Sung-kyun Kang, Myoung-Jun Lee, and Inhyuk Moon, “Design of Robotic Hand with Tendon-Driven Three Fingers”, *International Conference on Control , Automation and Systems in COEX, Seoul, Korea*. Oct. 17-20, 2008.
- [9].Birglen, L., and Gosselin, C.M., “Kinetostatic Analysis of Underactuated Fingers”, *IEEE Transactions on Robotics and Automation*, Vol. 20, No. 2, pp. 211-221, April (2004).
- [10].Birglen, L. Laliberté,T., and Gosselin, C.M., “Robotic Hands”, *Springer Tracts in Advanced Robotics*, Springer-Verlag, Berlin, Heidelberg, (2008).
- [11].Holland J. H., “Adaptation in Natural and Artificial Systems”, Ann Arbor, University of Michigan Press, 1975.
- [12].Manual of Otto Bock, “Myoboch Arm Components”, 2006.
- [13].Cross N., “Engineering Design Method” John Wiley & sons Limited, 1989.
- [14].Won Y. Yang, Wenwu Cao, Tae S. Chung, and John Morris, “Applied Numerical Methods Using Matlab”, John Wiley & Sons, Inc., 2005.
- [15]. Cutkosky, M. R. “On Grasp Choice, Grasp Models, and the Design of Hands for Manufacturing Tasks”, *IEEE Trans. Robot.Autom.*, vol. 5, no. 3, pp. 269–279, Jun. 1989.

## NOTATIONS

Symbols	Definition	Units
$f$	Vector of the normal contact forces	N
$f_i$	Normal contact force on phalanx i	N
$f_a$	Actuation force	N
G	Numerical value for each property (want)	-
$I_{gs}$	Index of the grasp forces	-
$I_{mpf}$	Index of Maximum pinching force	-
$I_{per}$	Percentage of the stability that is achievable by full-phalanx grasps	-
$itr$	Number of generation	-
$J$	Lower triangular matrix characterizing the contact forces locations	mm
$k_i$	Contact forces locations on phalanx i	mm
$l_i$	Length of phalanx i	mm
m	Population size	-
$0_i$	Center of pulley i	-
$r_i$	Radius of pulley i	mm
$T_a$	Actuation torque	N.mm
$T$	Transmission matrix	-
$t$	Input torque vector	N.mm
$W$	Weighted value for each property (want)	-
$\theta_i$	Angle of phalanx i	Rad
$\delta$	Kronecker delta	-

**Table (1) Boundaries of parameters to optimize.**

Parameters	Minimum Values (mm)	Maximum Values(mm)
$l_1$	40	55
$l_2$	20	32
$l_3$	15	25
$r_1$	3	12
$r_2$	3	11
$r_3$	3	11
$r_4$	3	8
$k_1$	4	50
$k_2$	2	29
$k_3$	1.5	22.5

**Table (2) Table of Kepner-tregos method.**

Solutions	Importance	Weight W	Sol.1		Sol.2		....		Sol. n	
Objectives			G	G×W	G	G×W	G	G×W	G	G×W
1 <sup>st</sup> criterion	Must		Go		No Go		Go		Go	
	Want	<b>W</b>	<b>G</b>	<b>G×W</b>	<b>G</b>	<b>G×W</b>	<b>G</b>	<b>G×W</b>	<b>G</b>	<b>G×W</b>
2 <sup>nd</sup> criterion		<b>0.60</b>			x	x				
3 <sup>rd</sup> criterion		<b>0.40</b>			x	x				
<b>ΣG.W</b>					x					
<b>Order</b>					x					

**Table (3) Optimal parameters of solutions 1, 2, 3, and 4.**

parameters	Sol. 1 (mm)	Sol. 2 (mm)	Sol. 3 (mm)	Sol. 4 (mm)
<b>l<sub>1</sub></b>	45.2	42.4	40	41.3
<b>l<sub>2</sub></b>	25.3	25	30.1	31.5
<b>l<sub>3</sub></b>	21.3	15	21.5	23.7
<b>r<sub>1</sub></b>	10.3	10.5	11.5	11.2
<b>r<sub>2</sub></b>	4	4	4.2	3.2
<b>r<sub>3</sub></b>	10.7	10.5	10.7	9.1
<b>r<sub>4</sub></b>	3.2	3	3	3.2
<b>k<sub>1</sub></b>	41.1	30.1	43.5433	8.80179
<b>k<sub>2</sub></b>	20.5	10.09	19.1021	14.0307
<b>k<sub>3</sub></b>	15.9	9.8	16.8486	17.661

**Table (4) Statistical comparison between solutions 1, 2, 3, and 4**

**(Sol. 1, Sol. 2, Sol. 3, and Sol. 4).**

	Sol. 1 (%)	Sol. 2 (%)	Sol. 3 (%)	Sol. 4 (%)
mean ( $f_1/fa$ )	9.9248	12.1676	11.6392	73.6945
mean( $f_2/fa$ )	7.9059	10.8142	8.9778	5.8967
mean( $f_3/fa$ )	7.5237	11.4286	6.9891	6.3715
s.d. ( $\frac{f_1+f_2+f_3}{fa}$ )	4.2222	9.2240	8.5759	11.1769
Percent stability	100	84	100	100
$I_{per}$	100	0	100	100
$I_{gs}$	255.4659	282.8038	237.1824	116.6475
$I_{mpf}$	25.35434	34.4104	27.60617	85.9627

**Table (5) Decision making Kepner-tregos method.**

Solutions	Importance	Weight W	Sol.1		Sol.2		Sol.3		Sol.4	
Objectives			G	G×W	G	G×W	G	G×W	G	G×W
1 <sup>st</sup> criterion	Must		Go		No Go		Go		Go	
2 <sup>nd</sup> criterion		0.6	85	51	-	-	79	47.4	39	23.4
3 <sup>rd</sup> criterion		0.4	10	4	-	-	10.7	4.3	33.3	13.3
$\Sigma G.W$			55		-		51.7		36.7	
Order			1 <sup>st</sup>		-		2 <sup>nd</sup>		3 <sup>rd</sup>	

**Table (6) Comparison of the parameters between solution 1 and solution 1 modified.**

Parameters	Solution 1 (mm)	Solution 1 modified. (mm)
$l_1$	45.2	45
$l_2$	25.3	25
$l_3$	21.3	20
$r_1$	10.3	10.5
$r_2$	4	4
$r_3$	10.7	10.5
$r_4$	3.2	3
$k_1$	41.1	40
$k_2$	20.5	20
$k_3$	15.9	15

**Table (7) Statistical comparison between solution 1 and solution 1modified.**

	Sol. 1 (%)	Sol. 1m (%)
mean ( $f_1/fa$ )	9.924746	10.40012
mean( $f_2/fa$ )	7.905937	8.366642
mean( $f_3/fa$ )	7.523658	7.619048
s.d. ( $\frac{f_1+f_2+f_3}{fa}$ )	4.222207	4.331663
Percent stability	100	100
$I_{per}$	100	100
$I_{gs}$	255.4659	253.7067
$I_{mpf}$	25.35434	26.38581

Table (8) Decision making Kepner-Tregos method between solution 1and solution 1modified.

Solutions	Importance	Weight W	Sol.1		Sol.1mod.	
<b>Objectives</b>						
1 <sup>st</sup> criterion	Must		Go		Go	
	Want	W	G	G×W	G	G×W
2 <sup>nd</sup> criterion		0.60	85	51	8.46	50.74
3 <sup>rd</sup> criterion		0.40	10	4	10.2	4.09
<b>ΣG.W</b>			55		54.83	

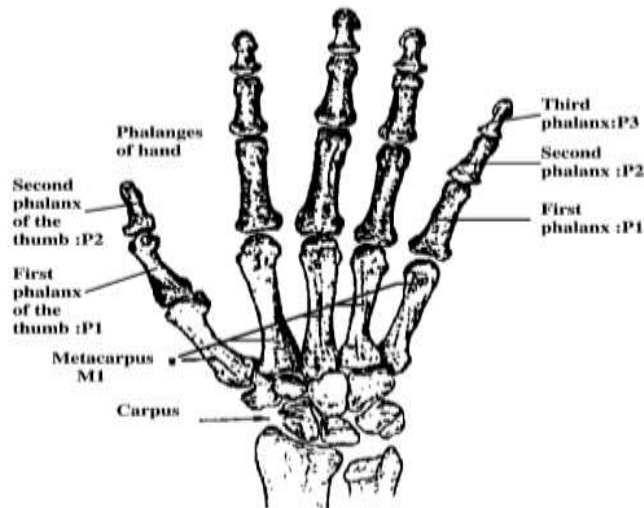


Figure (1) Physiology of a human hand [1].



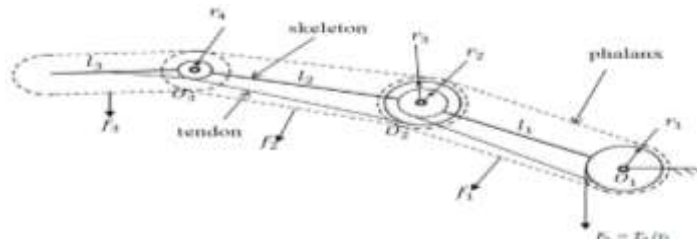


Figure (2) Three-phalanx finger using tendons.

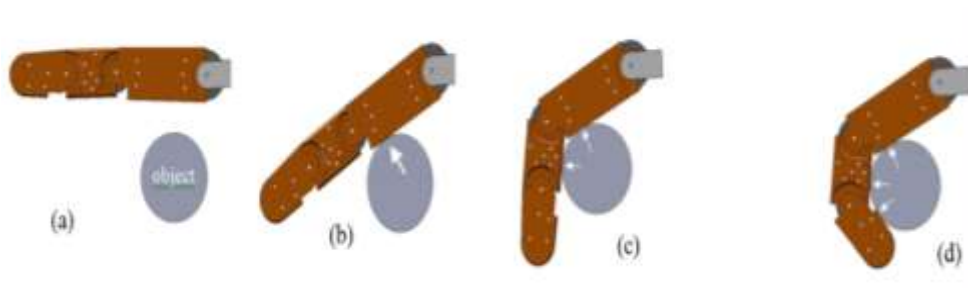


Figure (3) Ideal grasping sequences: (a) reaching phase, (b) first phalange in contact, (c) the torsion of the first spring allows the flexion of the PIP joint, and (d) after the contact with the second phalange, the torsion of the spring allows the flexion of the DIP joint and the encirclement of the object.

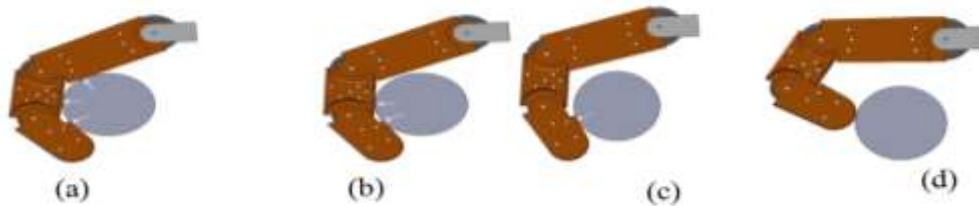


Figure (4) Degenerating into ejection, unstable designs can lead to the roll-back phenomenon, where the last phalanx slides against the object with a continuous closing motion resulting in a situation where the finger grasps nothing but itself, as shown in the sequence above, from (a) to (d) .

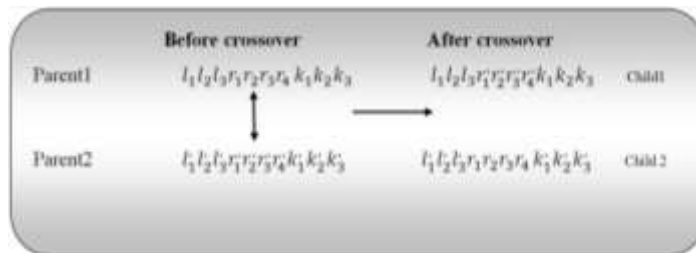
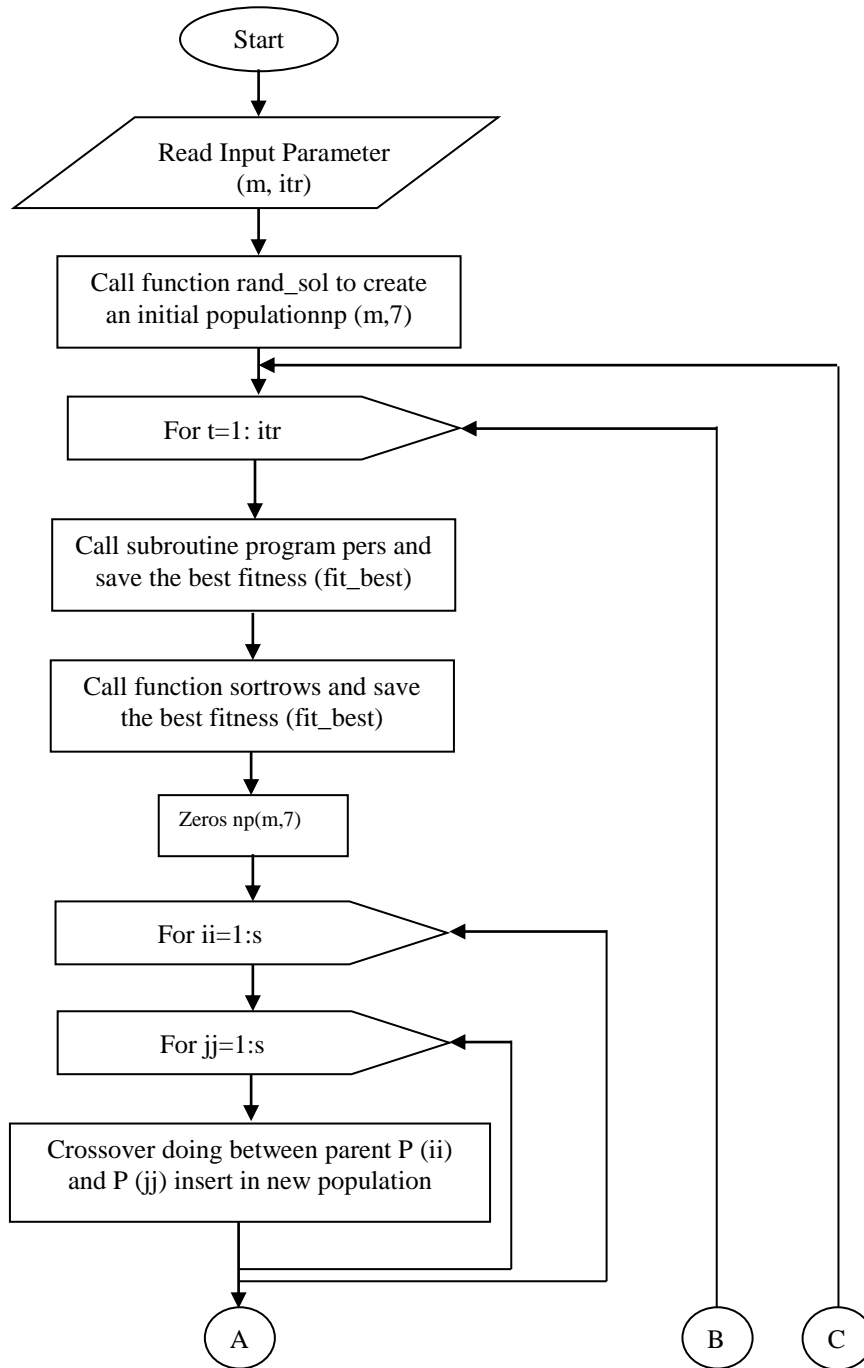


Figure (5) Two-point crossover.



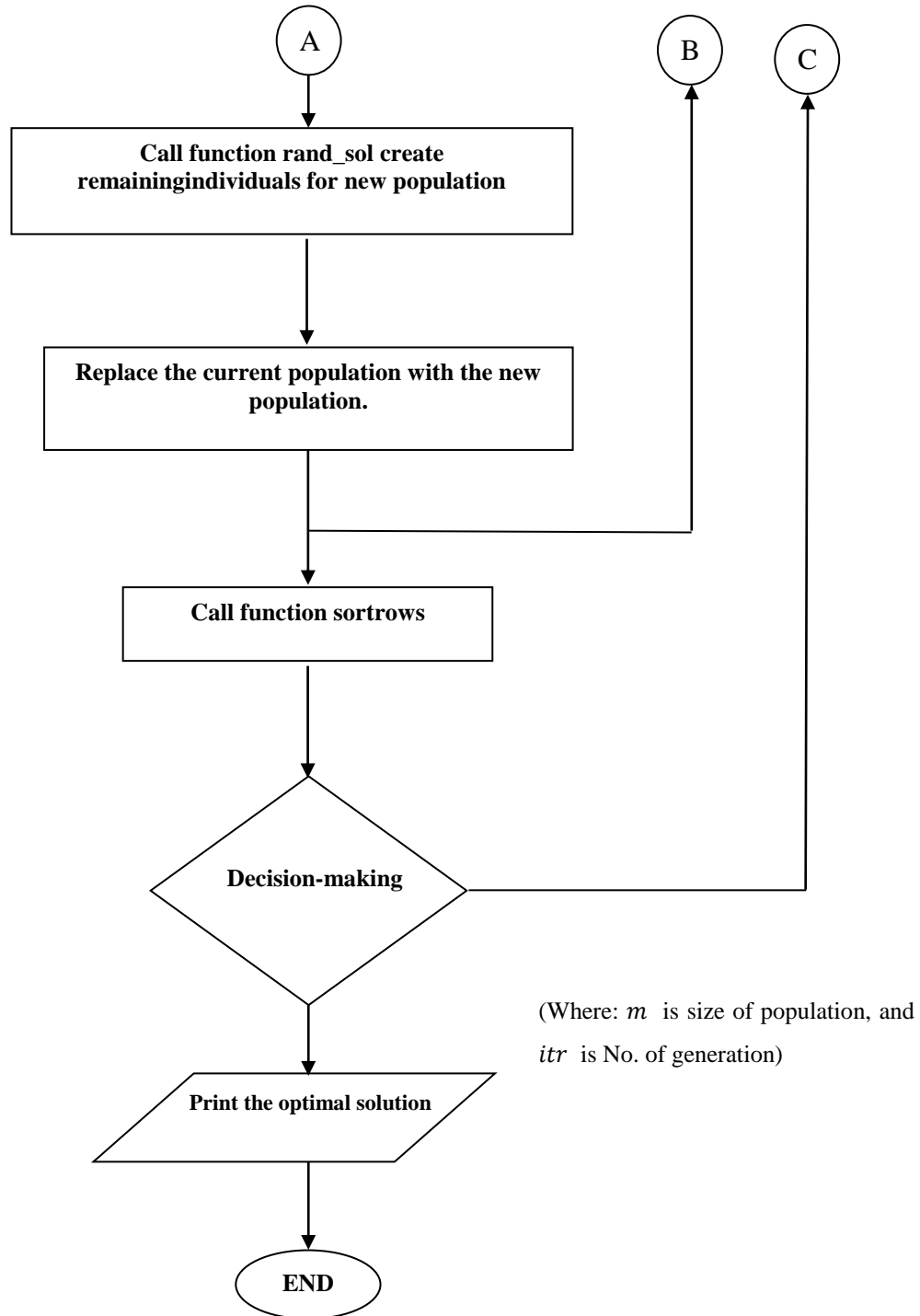


Figure (6): A flow chart of matlab optimization program for a prosthetic robotic hand.

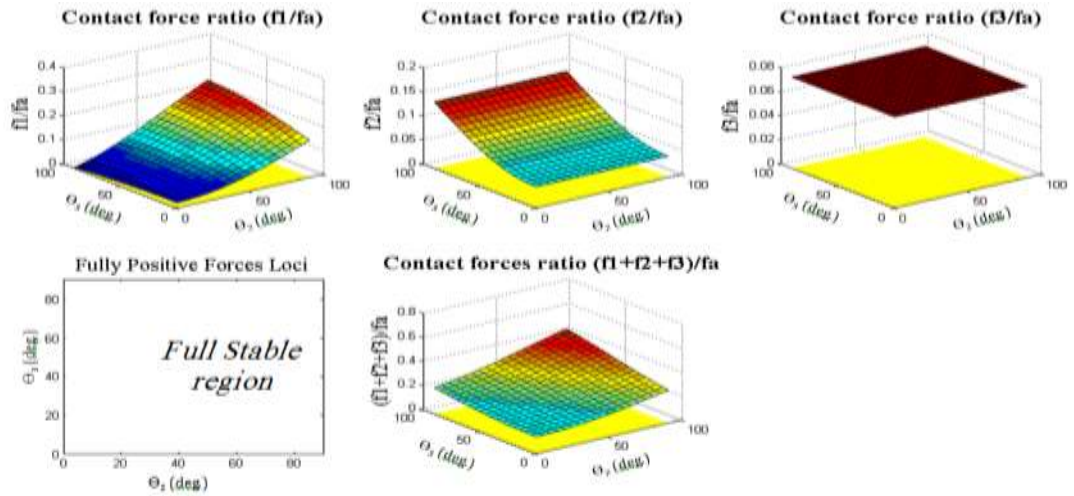


Figure (7) Contact forces ratio  $\frac{f_1}{f_a}, \frac{f_2}{f_a}, \frac{f_3}{f_a}, \frac{f_1+f_2+f_3}{f_a}$  and associated stability loci for solution 1. Each force component is shown with the zero plane  $f = 0$ , intersections with the latter are outlined.

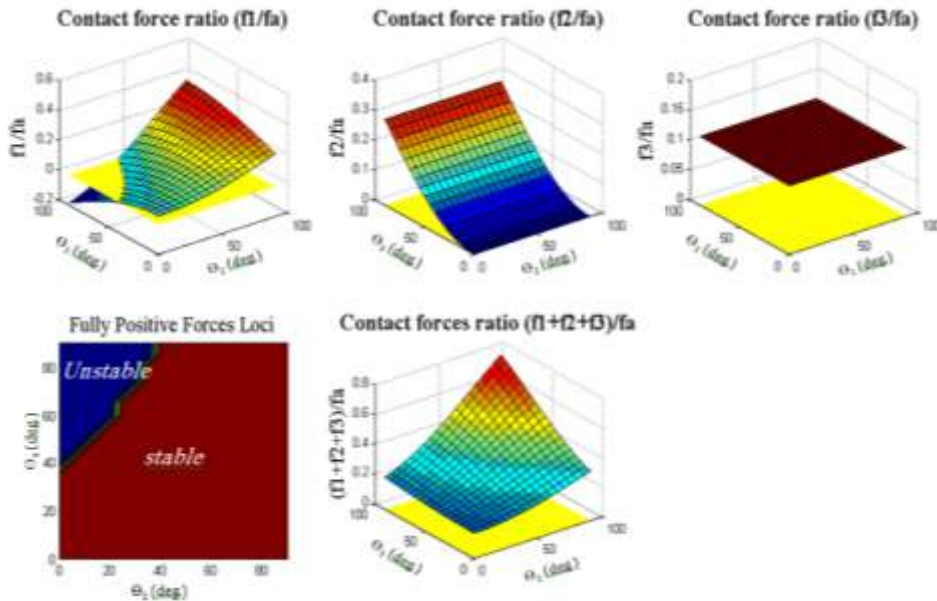


Figure (8) Contact forces ratio  $\frac{f_1}{f_a}, \frac{f_2}{f_a}, \frac{f_3}{f_a}, \frac{f_1+f_2+f_3}{f_a}$  and associated stability loci for solution 2. Each force component is shown with the zero plane  $f = 0$ , intersections with the latter are outlined.

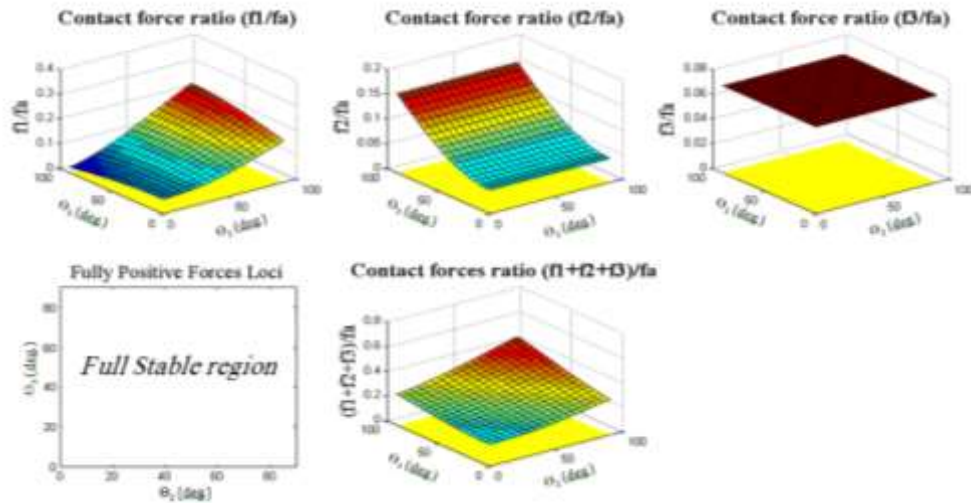


Figure (9) Contact forces ratio  $\frac{f_1}{fa}, \frac{f_2}{fa}, \frac{f_3}{fa}, \frac{f_1+f_2+f_3}{fa}$  and associated stability loci for solution 3. Each force component is shown with the zero plane  $f = 0$ , intersections with the latter are outlined.

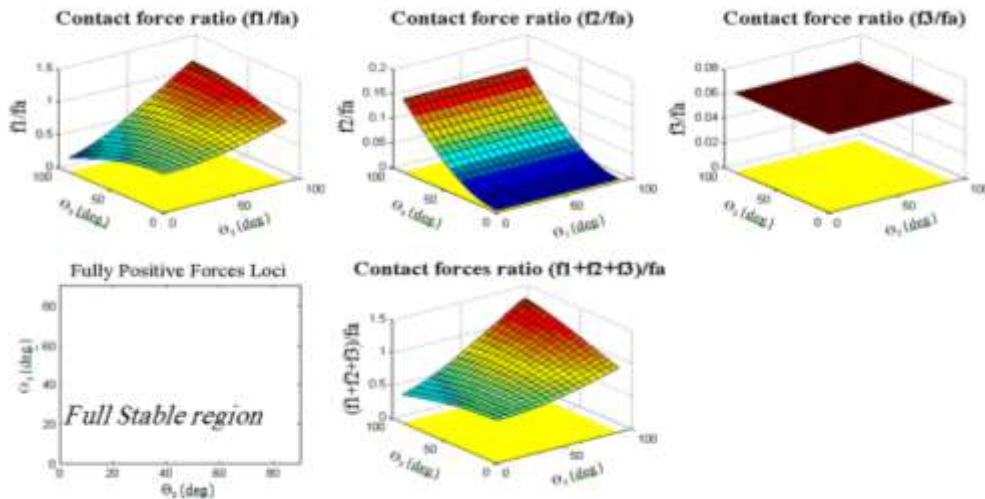
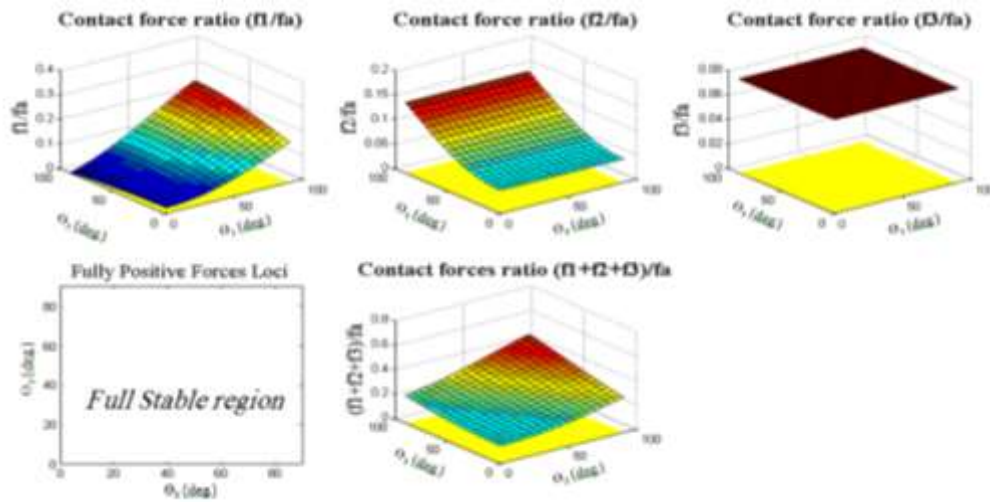


Figure (10) Contact forces ratio  $\frac{f_1}{fa}, \frac{f_2}{fa}, \frac{f_3}{fa}, \frac{f_1+f_2+f_3}{fa}$  and associated stability loci for solution 4. Each force component is shown with the zero plane  $f = 0$ , intersections with the latter are outlined.



Figure(11) Contact forces ratio  $\frac{f_1}{f_a}, \frac{f_2}{f_a}, \frac{f_3}{f_a}, \frac{f_1+f_2+f_3}{f_a}$  and associated stability loci for solution 1modified. Each force component is shown with the zero plane  $f = 0$ , intersections with the latter are outlined.



PC

3D Printers machine

Figure (12) 3D Printing machine.

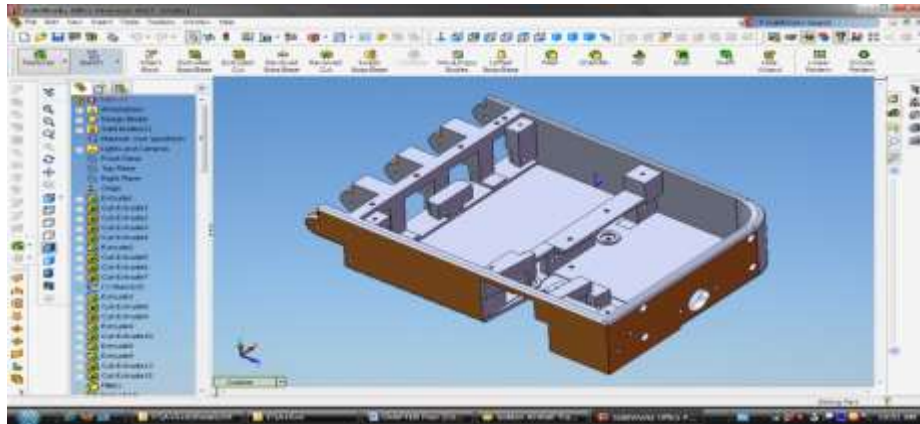


Figure (13) Model design by using Solid work software. (Palm component).

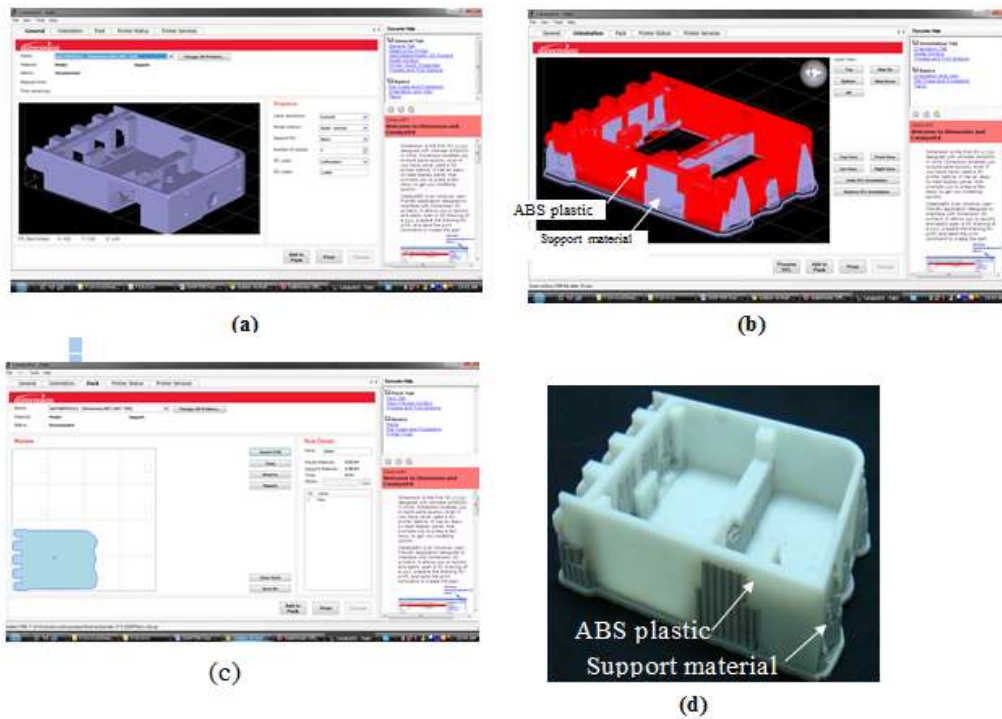


Figure (14) The palm component prototypes developed were built of ABS plastic using rapid prototyping technique. (a) STL files are imported Solid work program into Catalyst® EX Software, (b) Catalyst® EX Software creates necessary support structures, (c) Position of palm component in pack of 3D Printer, (d) Actual palm component made of ABS plastic.

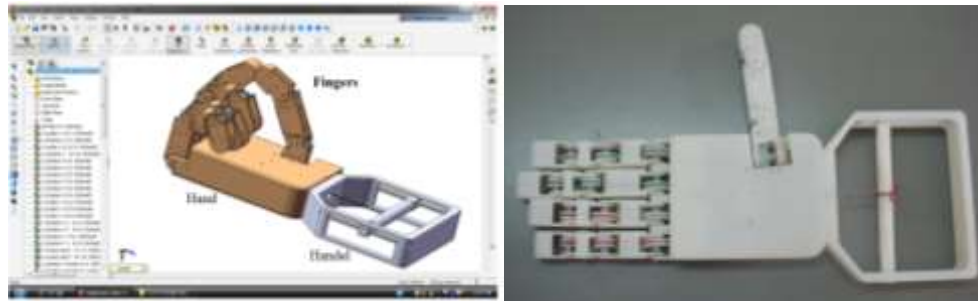


Figure (15) Prototype (CAD model and photograph) of the 15-dof underactuated hand.



Figure (16) A series of grasping experiments that were performed with the hand prosthesis.